

FEM Modelling of the Continuous Combined Drawing and Rolling Process for Severe Plastic Deformation of Metallic Materials

C. J. Luis, D. Salcedo, R. Luri, J. León and I. Puertas

Abstract In the last years, new severe plastic deformation (SPD) processes have been developed in order to produce very high values of deformation in the materials to be processed, with only small changes in the size of parts. This is not possible through conventional thermo-mechanical processes, in which the increase up to the above-mentioned values of deformation is usually associated with a change in their geometry. As is well-known, with enough accumulation of plastic deformation, a new submicrometric or even nanometric grain structure substitutes the former. Given that the grain size in metallic materials has a great deal of influence on their mechanical properties, the refinement of this grain size provides enormous technological advantages. For instance, at low values of temperature, a fine grain size can increase mechanical strength, hardness, fracture toughness and the material fatigue limit. Furthermore, at high values of temperature, the alloys with an ultrafine grain size may exhibit a superplastic behaviour and thus, the ability to undergo very high values of deformation with no damage to the material. The continuous combined drawing process in angular channels (CCDR) is a new concept of severe plastic deformation process (SPD), developed by researchers belonging to the Public University of Navarre and based on the patent (ES 2224787). In the present work, finite element analysis will be employed in order to study not only the strain

C. J. Luis (✉) · D. Salcedo · R. Luri · J. León · I. Puertas
Mechanical, Energetics and Materials Engineering Department, Public University
of Navarre, Campus de Arrosadia s/n 31006 Pamplona, Spain
e-mail: cluis.perez@unavarra.es

D. Salcedo
e-mail: daniel.salcedo@unavarra.es

R. Luri
e-mail: rodrigo.luri@unavarra.es

J. León
e-mail: javier.leon@unavarra.es

I. Puertas
e-mail: inaki.puerta@unavarra.es

distribution in the processed materials but also the homogeneity of the introduced strain. Moreover, experimental results will be compared to that obtained by using FEM. With the present work, it will be shown that it is feasible to achieve a process with possible industrial application, making the continuous processing of metallic materials in angular channels by SPD possible.

Keywords SPD · CCDD · FEM

1 Introduction

In this chapter, the results obtained by the finite element method of the so-called continuous combined drawing and rolling (CCDD) are shown by means of using several process conditions and types of materials. This process is a new concept of severe plastic deformation processes (SPD), developed by researchers belonging to the Public University of Navarre and based on the patent (ES 2224787) [1].

As can be observed in the state-of-the-art works recently published, a growing tendency exists in these last years towards the development of processes which make it possible to introduce very high values of plastic deformation within the materials to be processed with no significant change of their cross-section. This is not possible through conventional thermo-mechanical processes, in which the increase until the above-mentioned values of deformation is usually associated with a change in their geometry [2–5].

The aim of introducing very high values of plastic deformation within the processed materials is to achieve the appearance of a new submicrometric or even nanometric grain structure which will gradually substitute that existing initially, where this fact is favoured by an increase in the temperature of the process. Moreover, the fact of achieving a submicrometric structure presents several technological advantages, as this will have a direct influence on the mechanical properties of the new so-processed materials. For instance, at low values of temperature, a fine grain size can increase mechanical strength, hardness, fracture toughness and the material fatigue limit. Furthermore, at high values of temperature, the alloys with a ultrafine grain size may exhibit a superplastic behaviour and thus, the ability to undergo very high values of deformation with no damage for the material [6, 7].

Nevertheless, few processes which are able to take advantage of the benefits of the plastic deformation in angular channel exist, which could indicate the technological difficulty associated with the development of a process capable of operating continuously in order to impart high values of plastic deformation to metallic materials by means of an angular channel.

Among the discontinuous severe plastic deformation (SPD) techniques that have been developed in the last years to manufacture massive materials with submicrometric or even nanometric grain size, the first and more widely known is the Equal Channel Angular Extrusion or Pressing (ECAE or ECAP), which was

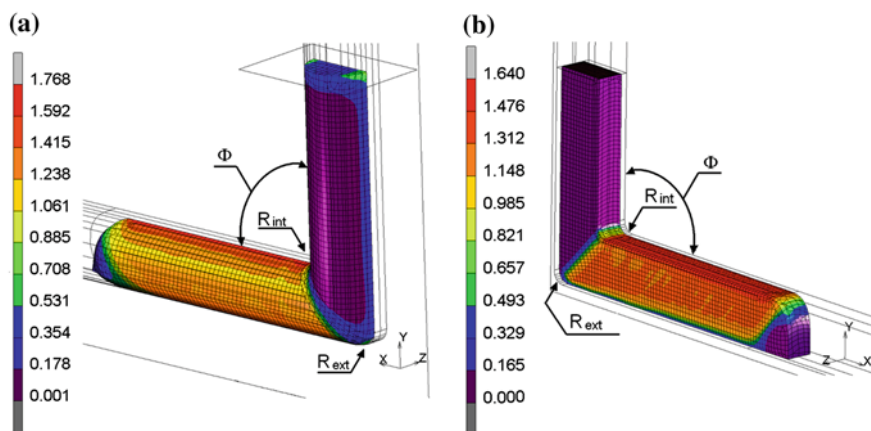


Fig. 1 Total equivalent plastic strain in the ECAE process **a** circular die, **b** square die

developed by Segal and his collaborators in the former Soviet Union, at the Institute for Metals Superplasticity Problems [8].

The angular channel extrusion consists in the compression of the billet of a material through a die with two channels which intersect at an angle varying generally between 90° and 135° , where the billet is extruded through the exit channel and this is the same size as the entrance channel. Figure 1 shows a finite element simulation of the ECAE process considering circular and square cross-section. When the material crosses the intersection between the two channels of the die, this undergoes a very intense shear plastic deformation ($\varepsilon > 1$) in a single passage. The material can be deformed with no fracture up to ($\varepsilon > 1$) due to the high value of hydrostatic pressure which exists inside the die channels when the extrusion process is carried out [9].

Although it is possible to achieve deformation values similar to those obtained in ECAE ($\varepsilon > 1$) by means of other conventional plastic deformation processes, such as drawing or rolling, the final values of section or thickness are reduced significantly, as such deformation increase is associated with a geometrical change. If it is taken into consideration that the ECAE process can be repeated several times as the part dimensions do not change, it is possible to accumulate a higher value of deformation, that is ($\varepsilon \gg 1$), which is translated into the fact that if it is intended to reach by conventional thermomechanical processes similar deformation values, the final dimensions would be so small that this would limit its subsequent application as structural element, not being able even to perform it [10]. As a consequence of this, severe plastic deformation processes have a great deal of interest, as the accumulation of deformation inside the processed material is achieved with no significant change in its cross-section.

The ECAE process allows us to manufacture highly deformed materials with ultrafine grain size and free of residual porosity. The process has been applied to a large number of materials such as copper, nickel, aluminium alloys and steel,

among others [3, 8–37]. With the ECAE process, it is obtained that a new sub-micrometric or even nanometric grain structure substitutes the initial one. With this, materials with improved mechanical properties are obtained since, as is well-known, the grain size of a metal has a great deal of influence on the mechanical properties of the materials and its refinement provides important technological benefits. For instance, a fine grain size can increase not only mechanical resistance, hardness, fracture toughness and fatigue limit, at low temperature, but also, at high temperature, the ultrafine grain alloys can exhibit a superplastic behaviour being able to undergo very high values of deformation with no damage to the material [6, 7].

With respect to other SPD processes in angular channel, the following ones could be highlighted: Cyclic Extrusion Compression (CEC) [38, 39], where this process was proposed by Korbel and Richert [38], Cyclic Extrusion and Compression (CEC), denominated CECRE (C shape Equal Channel Reciprocating Extrusion) [40] and Twist Extrusion, developed by Akbari et al. [41], among others.

Regarding other SPD processes which do not use an angular channel, the following ones stand out: the combined process of high pressure and torsion (High Pressure Torsion or HPT) [18, 42–46], Repetitive Corrugation and Straightening (RCS) [47, 48] and the process denominated as Multipass Coin Forging (MCF), which is similar to RCS [49], except for the arrangement and the geometry of the dies.

In spite of the great interest that discontinuous SPD processes present, as they allow us to obtain nanostructured materials, their industrial applications have not been as remarkable as could be expected, being in this aspect the ECAE process the one that presents a higher number of applications, such as those carried out by Ferrase et al. [19], Valiev et al. [50], Zhu et al. [51], Latysh et al. [52] and Tanaka et al. [53], among others.

In relation to the rest of the above-mentioned discontinuous SPD processes, such as HPT or CGP, the fact that they are discontinuous and relatively low and that they present a high value of heterogeneity in the deformation along with the fact that the size of the processed parts is not high enough could be what has limited their industrial applications.

Although the ECAE process presents diverse applications, the length of the billets is limited due to the buckling the punch can undergo if values of length more than ten times the value of the material diameter are employed. Furthermore, the process velocity is low since the values for the strain rate are not very high and it is necessary to open and close the die each time a new extrusion is needed to be performed.

Although several industrial applications have been carried out with this process, its importance is not as great as could be expected taking into consideration the significant improvement the so-processed materials imply.

In the present work, finite element analysis will be employed in order to study not only the strain distribution in the processed materials but also the homogeneity of the introduced strain in the CCDR process [1]. With the present work, it will be shown that it is feasible to achieve a process with possible industrial application, making possible the continuous processing of metallic materials in angular channel by SPD.

2 Description of the CCDR Process

In the CCDR process (Continuous Combined Drawing and Rolling), based on the patent ES-2002-01163 [1], a pushing force is generated at the entrance of the die by the effect of two rolling mills, whereby this is combined with a drawing force. By means of this process, it is possible to manufacture continuous materials through severe plastic deformation in angular channels [1, 54, 55]. In these days, a prototype has been developed in the Public University of Navarre, based on the previous patent for the continuous processing of sheet.

Figures 2 and 3 show different configurations for the implementation of the patented process [1], depending on the requirement to manufacture sheet or wire and where the rolling mills are not drawn to scale.

As can be observed, a compression force is generated at the entrance of the die by the employment of rolling mills and, simultaneously to the rolling process, a drawing process exists by which a force drawing the material is developed at the exit of the angular channel die. As a consequence of this, the stress values required for the rolling process are reduced as the device at the exit will help the material to pass through the angular channel die. Moreover, between passage and passage, the sheet can be rotated in order to homogenise the deformation pattern which is obtained along the cross-section of the processed material.

Among the different possible CCDR set-ups, some of them are shown in the following figures. Sheet and cylindrical bars or with other types of cross-section can be processed. Depending on the type of material to be processed, diverse applications can be found. The most outstanding ones are as follows: rolled structural shapes, wires, shapes for diverse applications, plane sheet and substituting steel parts for parts made of high resistance aluminium with mechanical properties improved by the refinement of grain that will be mentioned below.

Figure 4 shows the development of the continuous process of plastic deformation by angular channel for manufacturing sheet, as was shown in the operation sketch from Fig. 2. As can be observed, it is a plastic deformation process by angular channel which operates continuously, avoiding the buckling problem associated with the ECAE process, which limited the size of the processed parts. Figure 5 shows the material obtained with the process that has been developed.

The process denominated as “Continuous processing of metallic materials by means of plastic deformation with polyangular channel”, based on the patent Pat. 2224787 [1] or, in English, Continuous Combined Drawing and Rolling (CCDR) was proposed by researchers from the Public University of Navarre in collaboration with the “Centro de Estudios e Investigaciones Tecnológicas” from Guipúzua. The patented process presents the novelty of combining an extrusion force with a pushing system, composed of rolling mills. By the combined action of both processes, it is possible to process material continuously through a die which presents a configuration with angular channel.

The novelty of the CCDR process [1] in comparison to other continuous developed SPD processes consists in combining a pushing system in addition to a

Fig. 2 Operation sketch of the CCDR process for manufacturing sheet [1]

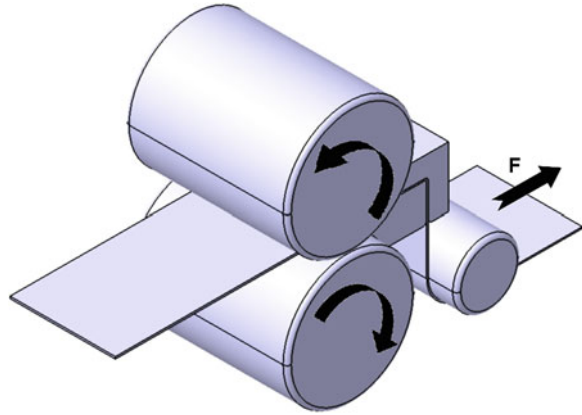
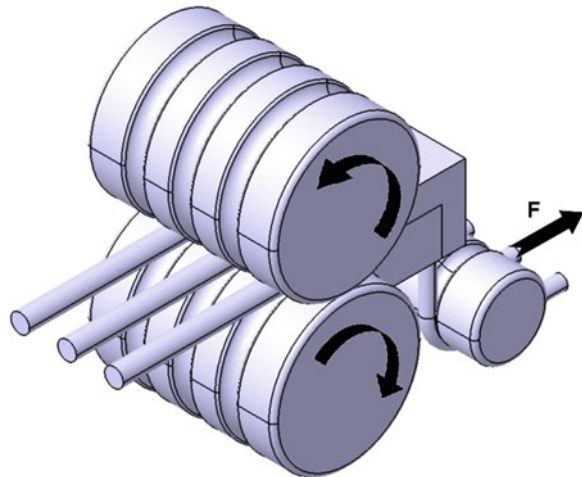


Fig. 3 Operation sketch of the CCDR process for manufacturing wire [1]



compression system that thus enables the material flow in the angular channel die, preventing the material from wrinkling at the entrance. Figures 2 and 3 show the fundamentals of the Continuous Combined Drawing and Rolling (CCDR). As can be seen in these figures, a compression force is generated at the entrance of the die by employing rolling mills and, simultaneously to the rolling process, a drawing process exists by which a force drawing the material is developed at the exit of the angular channel die. As a consequence of this, the stress values required for the rolling process are reduced significantly as the device at the exit will help the material to pass through the angular channel die. In this way, the wrinkling of the material is avoided at the entrance of the ECAE dies. With this process, it is possible to continuously manufacture materials through severe plastic deformation with an angular channel.

Figure 5 shows the material obtained with the process that has been developed. It is important to ensure that the material velocity at the exit is the same as the material velocity at the entrance of the die channel and, for this purpose, a series of



Fig. 4 Equipment developed for implementing a continuous process of plastic deformation by angular channel for manufacturing sheet, based on the patent proposed by Luis et al. (Pat. 2224787, 2002) [1]. The prototype is installed in the facilities of the Department of Mechanical, Energetics and Materials Engineering from the Public University of Navarre

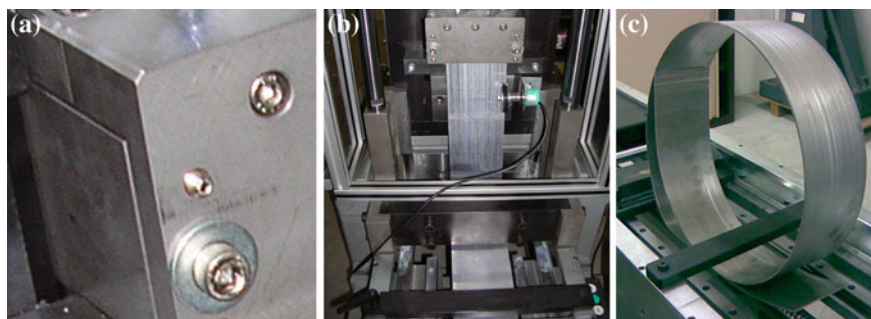


Fig. 5 View in detail of **a** the angular channel die, **b** measurement of the material velocity at the exit of the die, and **c** material processed by the CCDR equipment based on [1]

encoders are placed in order to determine the real velocity of the sheet. In this way, it is possible to regulate the CCDR process, not allowing the sheet to be stretched or wrinkled at the entrance of the die channel.

This equipment combines a rolling process with a drawing process, as is pointed out in Patent 2224787 [1]. In this way, the rolling mills are responsible for the force necessary to compress the material until the intersection of the die angular channel, whereby the gripping system has the aim of drawing the material at the exit of the die, in such a way that the material velocity at the entrance of the angular channel coincides with the material velocity at the exit of the latter. As a result, no significant necking of the processed material is produced.

In order to be able to control the sheet velocity at different points during the process, a series of measurement sensors have been installed. With the performance of these measurements, it is possible to modify via PC both the rolling or the drawing velocity, as convenient and in order to prevent not only a possible bulging of the material between the rolling mills and the die but also a drastic reduction of the material cross-section at the exit.

3 Finite Element Modelling

In the present section, some simulations performed on the CCDR process, presented in the previous section, are shown. In order to perform them, an aluminium alloy of type AA8011 has been selected. With the aim of analysing the processing of the material by CCDR through the use of finite element method (FEM), the process conditions that are shown in Table 1 have been selected. The sheet width was considered to be 130 mm and it was maintained constant in all the simulations.

With respect to the elements, their size is of 0.05×0.25 mm for the simulations with a single sheet and of 0.05×0.5 mm for those with two sheets. The dies have been meshed utilising division of curves and automesh with the option of advance front, making the zones which will undergo higher values of stress be meshed as fine as the sheet element so that situations of nodes penetration do not take place (0.05 mm). In the same way, it is very important that the nodes in contact are 10 or more so that the peaks in the values of force and stress, which are produced when the sheet is being processed, are as small as possible.

In Fig. 6, an image of the die mesh can be observed. Plane strain conditions have been employed as the sheet width is much higher than its thickness. This approach is good enough and it saves calculation time, in relation to that necessary to perform the simulation considering a tridimensional geometry.

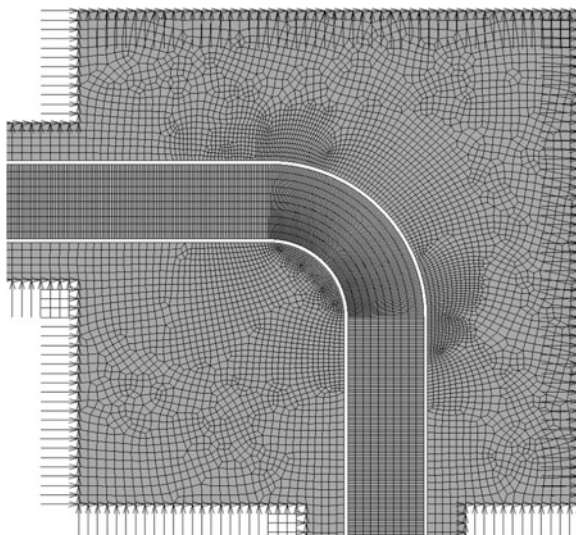
An element type Quad 4, which is a quadrilateral with four integration points, has been utilised. The number of elements is 54,000. As was previously-mentioned, plane strain conditions have been assumed since the sheet width is much higher than the sheet thickness.

With respect to the material employed in the FEM simulations, the aluminium alloy AA8011, whose flow stress is depicted in Fig. 7, has been selected.

In order to estimate the damage the sheet undergoes during the process, a model type Cockroft–Latham [56] has been taken into account. The damage threshold,

Table 1 Simulations performed

Sheet of 2.6 mm, rolling 2 mm, die channel 2.2 mm, internal radius 2 mm
Sheet of 2.6 mm, rolling 2 mm, die channel 2.2 mm, internal radius 1.5 mm
Sheet of 5.2 mm, rolling 4 mm, die channel 4.2 mm, internal radius 2 mm
Sheet of 5.2 mm, rolling 4 mm, die channel 4.2 mm, internal radius 1.5 mm
Sheet of 7.8 mm, rolling 6 mm, die channel 6.2 mm, internal radius 2 mm
Sheet of 7.8 mm, rolling 6 mm, die channel 6.2 mm, internal radius 1.5 mm
Two sheets, each one of 2.6 mm, rolling 4 mm, die channel 4.2 mm, internal radius 2 mm
Two sheets, each one of 2.6 mm, rolling 4 mm, die channel 4.2 mm, internal radius 1.5 mm
Three sheets, each one of 2.6 mm, rolling 6 mm, die channel 6.2 mm, internal radius 2 mm
Three sheets, each one of 2.6 mm, rolling 6 mm, die channel 6.2 mm, internal radius 1.5 mm

Fig. 6 Meshing of both angular channel die and processed material

which is the deformation value from which the damage is considered to start, has been selected as zero, that is to say, the damage is considered to begin when the material is deformed.

In relation to the contacts employed, except for the case of the sheets and the dies, which are all deformable bodies, the rest of the bodies used in the simulations are considered to be rigid. Figures 8 and 9 show the contacts that are taken into account in the performed simulations.

The velocity of the process is 20 mm/min and the rolls rotate at 0.004 rad/s. It is important to point out that the drawing velocity is slightly higher than the velocity of the rolls in order to avoid the buckling of the material at the entrance of the angular channel dies.

Regarding the contacts, a distance tolerance of 0.0025 mm is considered to detect the contact situation and a bias factor of 0.9 for the sensibility of a rigid

Fig. 7 AA8011 flow stress

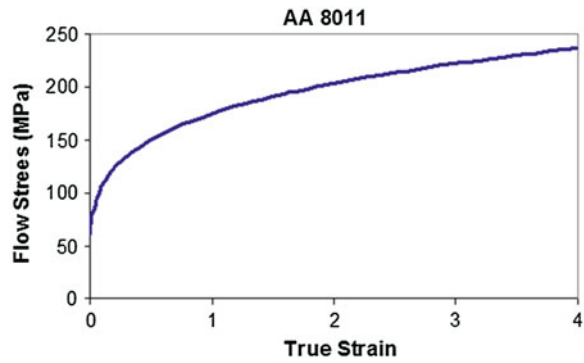


Fig. 8 Contacts die-material

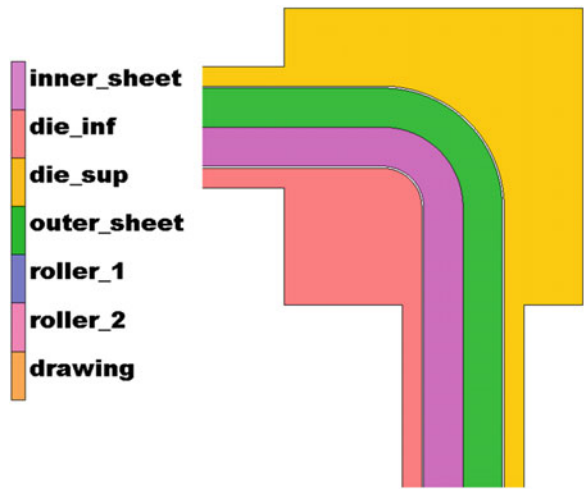
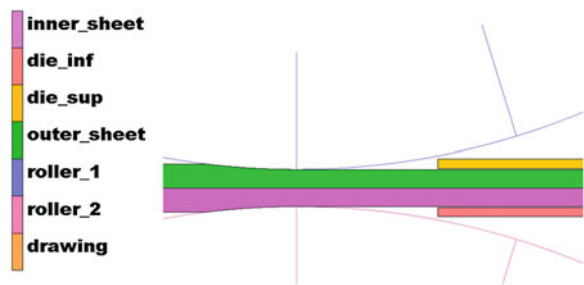
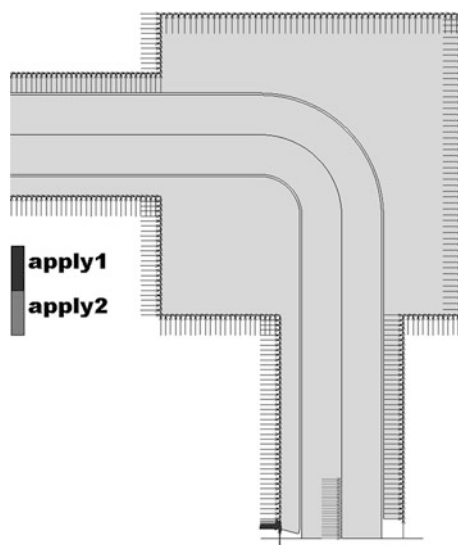


Fig. 9 Detailed view of the contacts in the rolling



body to be crossed and of 0 when there is a contact between deformable bodies (0 means that when the contact is detected, the interval fixed by the distance tolerance is symmetric, which this is very useful when the bodies in contact are

Fig. 10 Detailed view of the angular channel die



both deformable). Moreover, the initial stress in the contacts is not taken into account in order to avoid subsequent problems.

The friction model employed is that of type Shear [57], with a velocity of relative displacement of 0.025 mm/s. The values for the friction coefficients are as follows: 0.1 between sheets; 0.9 between the rolls and the sheet, and 0.1 between the dies and the sheet. The body which draws from the sheets is glued to an end of the latter.

The detection method for the contact between deformable bodies (useful in the case of two sheets and in the case of one sheet against any of the dies) is double sided, that is, it checks the contact at the nodes of the two bodies, which slows the simulation but is essential for the good running of this. The criterion of separating the nodes from the lines which limit the rigid bodies is considered through the relative stress, where if this changes the 0.1 %, the nodes are separated from the rigid body.

When the dies model is changed from a static rigid body to a deformable body, it is necessary to introduce restrictions in the nodes in order to avoid their displacements. Restriction of movement in axes “x” and “y” is applied to the external nodes of the dies. As well as this boundary condition, in the simulations performed with more than one sheet, a restriction of movement in axis “x” is applied to the first nodes in contact with the rigid body, which model the tension force exerted over the sheet at the exit of the angular channel. Figure 10 shows the previously mentioned boundary conditions as “apply1” and “apply2”, respectively.

The iterative process employed to linearise the problem is the full Newton–Raphson method [57] with 50 possible recycles and with the possibility to continue the calculation although non-positive definite matrices appear. In order to solve the equations in each step of the simulations, direct sparse is utilised. The convergence

of each iteration is achieved with residuals or displacements with a tolerance of 0.1 % in the values for the force and for the relative displacement.

The results presented are the equivalent plastic deformation, the von Mises stress, the stress tensor, the damage according to the Cockroft–Latham’s model and the equivalent elastic deformation. For high values of deformation, the simulations are performed using both the Lagrange’s method and the additive decomposition option for the plastic zone.

4 Finite Element Results

In the present section, the main results obtained in relation to the plastic deformation exerted on the material, the accumulated damage, the stresses in the die and the values for the force are assessed employing the FEM simulation software Marc Mentat 2008TM.

4.1 Total Equivalent Plastic Strain

The aim of the CCDD process is to impart to the processed material high values of deformation with no significant change of its cross-section, in such a way that it is possible to accumulate higher deformation values. In the present section, the results obtained regarding the accumulation of plastic deformation inside the processed sheet are shown.

As was above-mentioned, by CCDD, the cross-section is reduced slightly in order to prevent the sheet from being accumulated at the entrance of the die. The temperature is being applied to the process to ensure that the section does not vary as it is possible to work with similar velocities of pushing and drawing. In addition to this, it is possible to reduce the heterogeneity that appears when the material is processed twice using route C between passes, where this route consists in rotating 180° the processed sheet in such a way that the zone which is first in contact with the inner radius of the die is in the next passage in contact with the outer radius, thus increasing the deformation exerted on the material and its homogeneity. This has not been included in this chapter because it does not form part of its objectives but it will be shown in a future technical work.

The values for the plastic deformation accumulated in the material as a consequence of the rolling and of the deformation in the angular channel have been assessed. A comparison of the deformation in the same sheet has been made when the inner radius and the sheet thickness vary. Moreover, the deformation values when a single sheet or when various sheets with the same thickness of the latter pass through the same die. In the images shown in Fig. 11a–g, the deformation imparted to the material can be observed when modifying the process conditions.

Taking the obtained results into account, the deformation diminishes when the internal radius of the lower die (R_{int}) is increased.

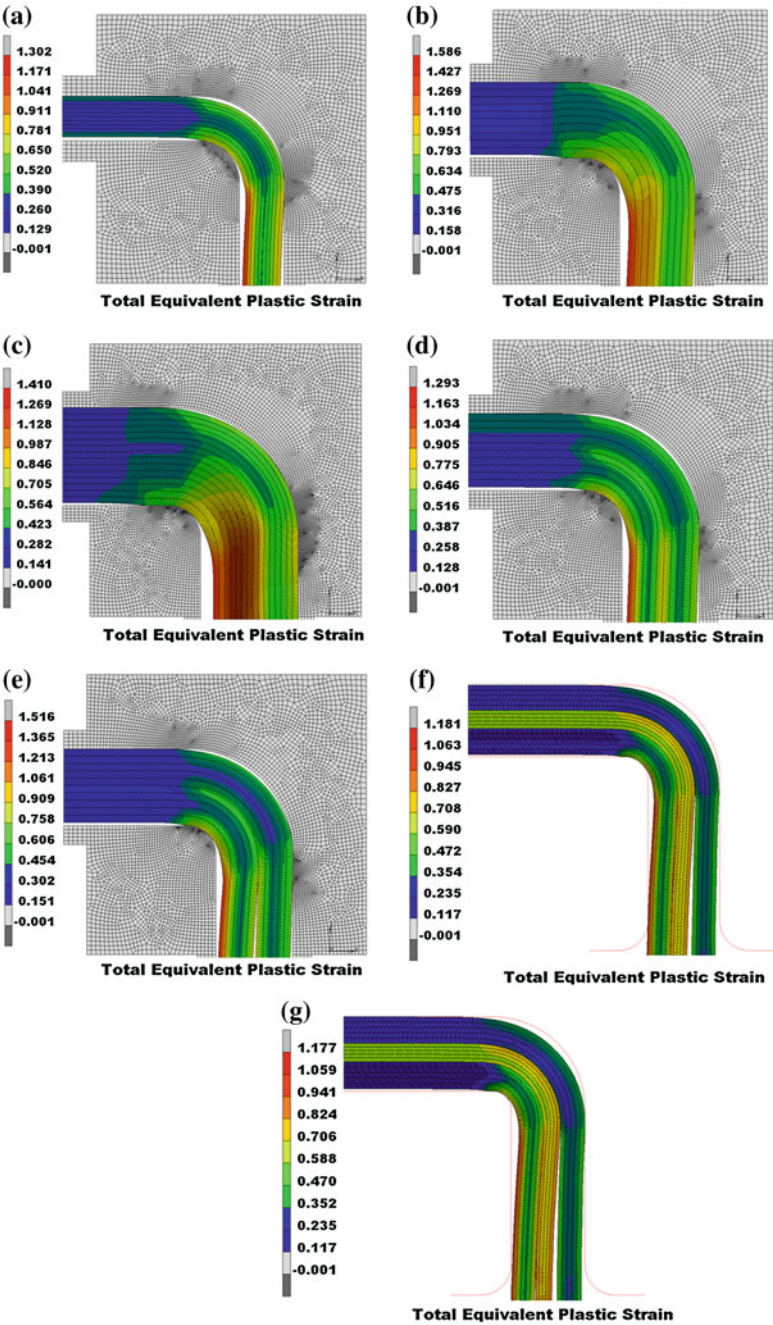
In the case of Fig. 12a, corresponding to a sheet of 2.6 mm thickness rolled up to 2 mm, it can be observed that the deformation obtained with the lowest inner radius is always higher than that obtained with the highest inner radius. The maximum value is located at the zone closer to the inner radius, a decrease is observed in the central zone and a new increase at the other end of the sheet. For 2 mm, the maximum value is of 1.3 whereas in the case of the inner radius 1.5 mm, the deformation value is of 1.5, which means a 15 % higher. Figure 12b, which is the case of one sheet of 5.2 mm thickness rolled up to 4 mm, shows that the deformation has a pattern similar to the previous case. The difference between the deformation obtained with the different radii is lower. The maximum value is attained for the radius of 2 mm although it is the intermediate zone of the sheet where a higher value of deformation is observed when a lower inner radius is used. Furthermore, Fig. 12c shows the deformation of one sheet of 7.8 mm thickness rolled up to 6 mm and later on, processed by CCDR. As can be observed, when the internal radius of the angular channel die is decreased, the achieved value of deformation is higher.

In order to analyse if there exists a change in the deformation imparted when a higher number of sheets with the same thickness is processed simultaneously, the simulations previously shown were performed, whose comparison is depicted in Fig. 13. In the study case for the three sheets, the existence of hydrostatic pressure in the central sheet was considered in order to diminish the damage and to increase the deformation value. In the following graphs, the attained results are shown.

In Fig. 13a and b, it can be observed that the deformation with a single sheet is always higher than that in the case of two sheets with the equivalent section. A border effect is seen in the case of the sheets processed simultaneously but it is not enough to improve that obtained with a single sheet of processed material. The same behaviour can be observed in Fig. 13c and d. Both inner and outer sheets provide deformation values much lower than those attained when a single sheet is processed. On the contrary, the intermediate sheet has deformation values similar to those obtained with a single sheet, presenting the advantage of having a much higher homogeneity of plastic deformation. Nevertheless, it can be seen that the central sheet reduces its section more than both, the internal and the external ones, as can be observed in Fig. 11g.

The thickness of the processed sheet is important for the possible applications of the material processed by CCDR. Figure 14a and b show the deformation values attained for sheets with a starting thickness of 2.6, 5.2 and 7.8 mm.

As can be observed in Fig. 14a and b, when the thickness is increased, the homogeneity and the mean deformation in the section increase. The maximum value is achieved for the sheet with an intermediate value of thickness although it seems that the sheet with the highest thickness presents a decrease in the central zone of a lesser degree.



◀ **Fig. 11** Accumulated value of plastic deformation inside the material when varying the CCDD process conditions. **a** CCDD simulation (increment 1,500) in a die with an inner radius of 2 mm and one sheet with a thickness of 2 mm after rolling. **b** CCDD simulation (increment 1,500) in a die with an inner radius of 2 mm and one sheet with a thickness of 4 mm after rolling. **c** CCDD simulation (increment 1,500) in a die with an inner radius of 2 mm and one sheet with a thickness of 6 mm after rolling. **d** CCDD simulation (increment 1,500) in a die with an inner radius of 2 mm and two sheets with a thickness of 2 mm after rolling. **e** CCDD simulation (increment 1,500) in a die with an inner radius of 1.5 mm and two sheets with a thickness of 2 mm after rolling. **f** CCDD simulation (increment 1,650) in a die with an inner radius of 2 mm and three sheets with a thickness of 2 mm after rolling. **g** CCDD simulation (increment 1,650) in a die with an inner radius of 1.5 mm and three sheets with a thickness of 2 mm after rolling

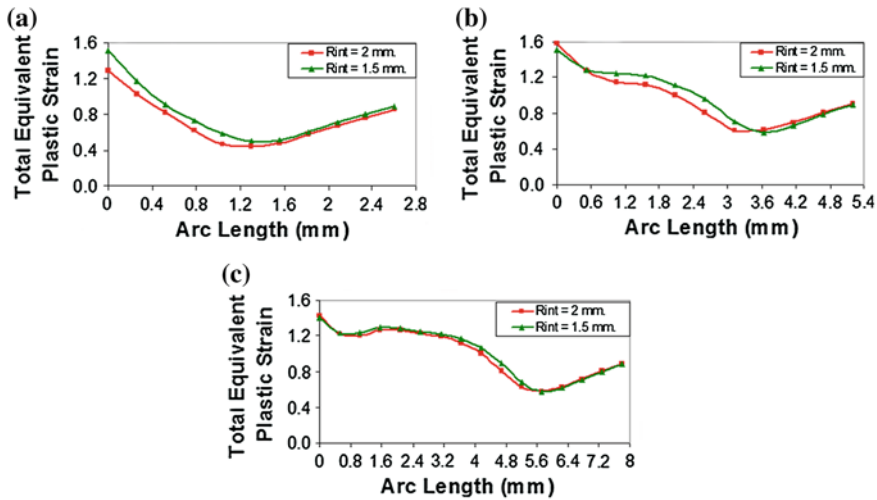


Fig. 12 Plastic deformation in a section of the sheet. **a** Deformation pattern of one sheet with a thickness of 2 mm after rolling. **b** Deformation pattern of one sheet with a thickness of 4 mm after rolling. **c** Deformation pattern of one sheet with a thickness of 6 mm after rolling

4.2 Analysis of the Damage Imparted to the Processed Material

Although with the CCDD process it is intended to impart very high values of plastic deformation to the processed materials, it is essential that the imparted damage is as low as possible in order to diminish the appearance of cracks limiting the subsequent applications of the processed material.

The damage is the progressive process by which the materials break subjected to a specific load. In a microscale level, this is the accumulation of microstresses in the neighbourhood of defects and the breaking of bonds, which generates micro-cracks that initiate one crack [58]. Damage is not an observable variable and a model definition is required in order to measure it [59]. Different approaches have

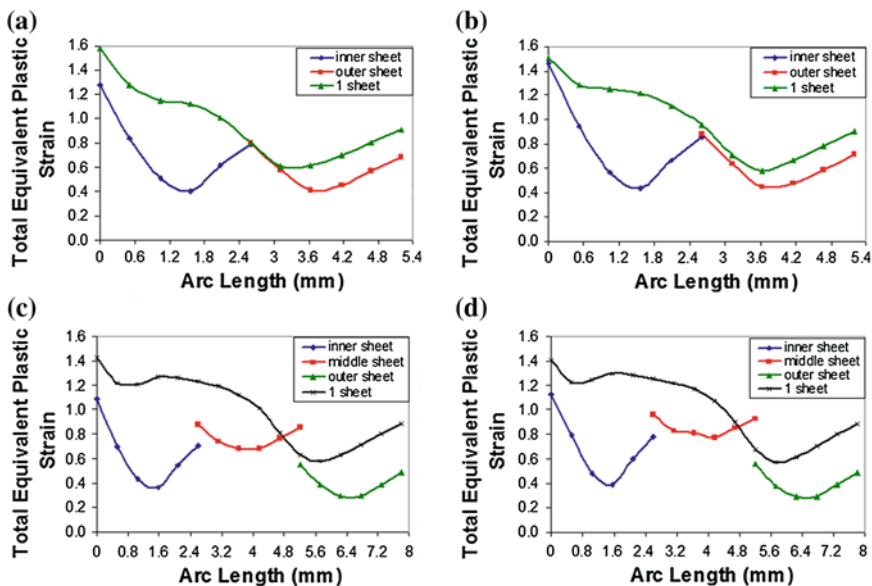


Fig. 13 Plastic deformation in the sections of the sheets. **a** Deformation pattern of one sheet of 4 mm thickness after being rolled versus two sheets processed simultaneously each one of 2 mm thickness with an inner radius of 2 mm. **b** Deformation pattern of one sheet of 4 mm thickness after being rolled versus two sheets processed simultaneously each one of 2 mm thickness with an inner radius of 1.5 mm. **c** Deformation pattern of one sheet of 6 mm thickness after being rolled versus three sheets processed simultaneously each one of 2 mm thickness with an inner radius of 2 mm. **d** Deformation pattern of one sheet of 6 mm thickness after being rolled versus three sheets processed simultaneously each one of 2 mm thickness with an inner radius of 1.5 mm

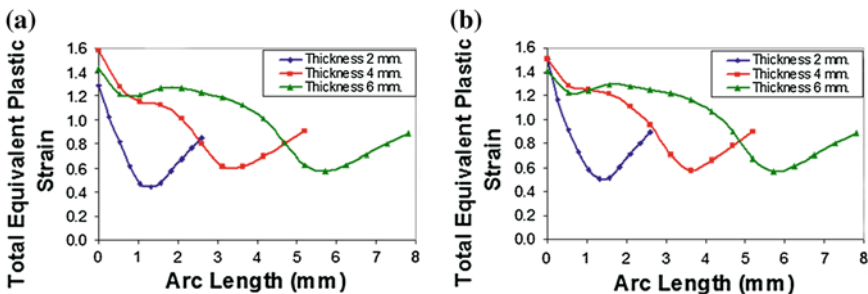


Fig. 14 Plastic deformation in the sections of the sheets with different thickness. **a** Deformation pattern of one sheet of 2 mm thickness after being rolled. **b** Deformation pattern of one sheet of 4 mm thickness after being rolled

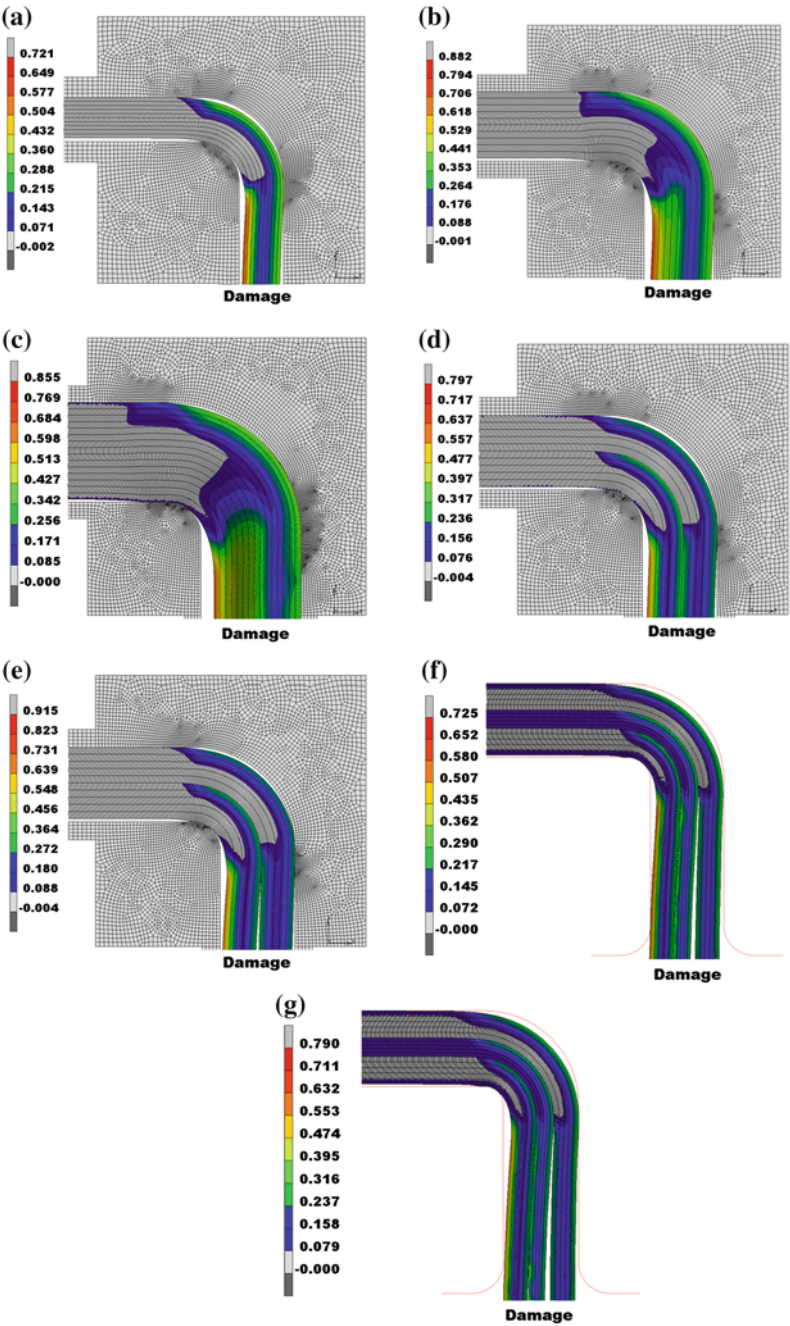
been proposed in order to determine the damage mechanics [60–64]. All these formulations have been classified in the three main approaches in [65]: abrupt failure criteria, porous solid plasticity and continuum damage mechanics (CDM).

The first approach predicts the failure when one external variable, that is uncoupled from other internal variables, reaches its critical value. For the second approach, Gurson's type model was derived for porous materials taking into account only the nucleation and growth of the microvoids [60]. This formulation was extended later by other authors [66, 67]. In the last years, as is analysed in [65], a number of finite element unit cell based on micromechanical studies have been performed in order to correlate voids evolution and interaction with the resulting macroscale material yield function. The third approach assumes that the damage is one of the internal constitutive variables that accounts for the effects of the material constitutive response induced by the irreversible processes that occurs in the material microstructure [65]. The initial work in this field was developed by [61]. Subsequently, new models were developed such as those of: Lemaitre [62] and Chaboche [68]. In the last two decades a great number of CMD based formulations have been proposed as can be seen in the revision of Bonora [65]. The limitations of these CMD approaches were overcome with a new damage model formulation proposed in [69].

Although a large number of damage models exist, in the present work, the damage values in the CCDD process have been obtained by using Cockcroft–Latham damage models with the Marc MentatTM FEM software. This model is commonly used in SPD processes [70]. This will allow us to determine the most appropriate die geometry to perform the process. In the present section, the results of the FEM simulations for the damage exerted on the material are shown, as was mentioned, employing a model type Cockcroft–Latham [56]. This model can predict a zone of located damage through Eq. (1). Cockcroft and Latham damage model is a damage indicator which is often used to predict the initiation of the cracks. It considers the effects of the maximum principal tensile stress. The damage in Cockcroft–Latham model is calculated by using Eq. (1).

$$C = \int_0^{\bar{\epsilon}_f} \frac{\sigma_{\max}}{\bar{\sigma}} d\bar{\epsilon} \quad (1)$$

where $\bar{\epsilon}$ represents the equivalent plastic strain, $\bar{\epsilon}_f$ is the equivalent plastic strain just at the moment of fracture, σ_{\max} is the maximum principal tensile stress and C is material constant threshold for damage. As can be observed, no material parameters have to be employed in order to compare how the die geometries influence the damage, when Cockcroft–Latham damage model is used. In order to determine how the die geometry influences the damage on the processed material, different FEM models with the above mentioned conditions were simulated in order to calculate the Cockcroft–Latham damage parameter. The damage imparted to the material has been evaluated as a consequence of both the rolling process and the angular channel (Fig. 15).



◀ **Fig. 15** Damage exerted on the material. **a** CCDR simulation (increment 1,500) in a die with an inner radius of 2 mm and one sheet with a thickness of 2 mm after rolling. **b** CCDR simulation (increment 1,500) in a die with an inner radius of 2 mm and one sheet with a thickness of 4 mm after rolling. **c** CCDR simulation (increment 1,500) in a die with an inner radius of 2 mm and one sheet with a thickness of 6 mm after rolling. **d** CCDR simulation (increment 1,500) in a die with an inner radius of 2 mm and two sheets with a thickness of 2 mm after rolling. **e** CCDR simulation (increment 1,500) in a die with an inner radius of 1.5 mm and two sheets with a thickness of 2 mm after rolling. **f** CCDR simulation (increment 1,650) in a die with an inner radius of 2 mm and three sheets with a thickness of 2 mm after rolling. **g** CCDR simulation (increment 1,650) in a die with an inner radius of 1.5 mm and three sheets with a thickness of 2 mm after rolling

In this section, the effect of the inner radius on the damage imparted to the sheet is shown. The values of the die inner radius (R_{int}) for the cases studied are 2 and 1.5 mm.

Figure 16a shows the case of a sheet of 2.6 mm thickness rolled up to 2 mm. As can be observed, the model predicts that the damage exerted with a lower inner radius is always higher than that with a higher inner radius. The maximum value is given in the zone closer to the inner radius, followed by a decrease in the central zone and a final increase at the other end of the sheet.

In the zone close to the outer radius, the level of damage is similar in both cases but in the inner part of the sheet, the difference is remarkable, where with a radius of 1.5 mm, the damage is 33 % higher than in the case with an inner radius of 2 mm. Figure 16b shows that the difference between the damage exerted by the different values of radius is lower.

The maximum value is obtained for a radius of 2 mm but the intermediate zone of the sheet is more damaged with a lower value of radius. Figure 16c shows that there is no difference between the damage exerted on the inner zone and on the outer. When the inner radius decreases, the imparted damage is higher, specially for low values of sheet thickness. Moreover, when the sheet thickness is increased, the influence of the inner radius decreases.

In Fig. 17a and b, it can be observed that the damage when a single sheet is processed is higher than that for the two equivalent sheets in section, except in the contact zone of the two sheets, because of the border effect produced when both of them are processed simultaneously. Figure 17c and d show that the simultaneously processed sheets have values of damage lower than those attained in the single processed sheet. In the contact zone between the intermediate sheet and the outer, the level of damage exerted by the friction in these sheets exceeds the sheet with the highest value of thickness.

In the following graphs, Fig. 18, the values of damage for sheets with a starting thickness of 2.6, 5.2 and 7.8 mm, respectively, are shown. One can see that when the thickness is increased, the mean value of damage in the section increases.

The maximum value is achieved for the sheet with the intermediate value of thickness. In this case, it is interesting to employ sheets with a lower value of thickness in order to reduce the level of damage in the central part of the sheet. This result coincides with that obtained in the previous section, where it is shown

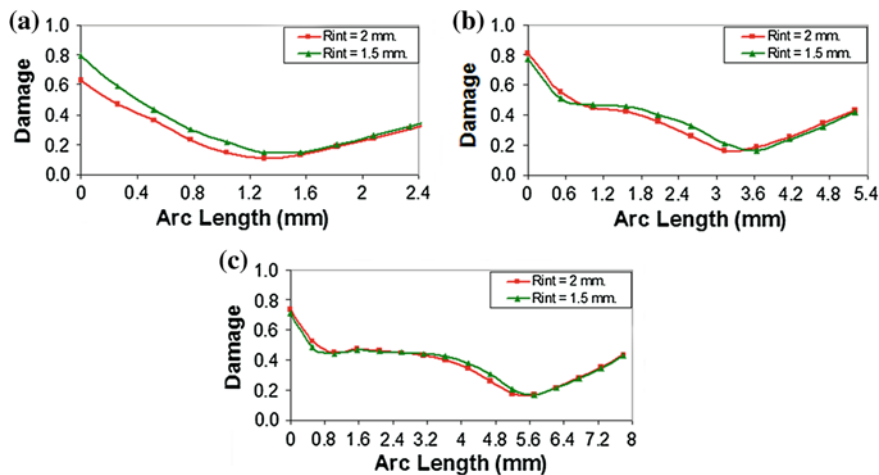


Fig. 16 Values of damage with Cockroft–Latham model in one section of the sheet. **a** Damage pattern for one sheet of 2 mm thickness after being rolled. **b** Damage pattern for one sheet of 4 mm thickness after being rolled. **c** Damage pattern for one sheet of 6 mm thickness after being rolled

that it is preferable to process several sheets of low thickness rather than a single sheet with a higher thickness.

4.3 Equivalent Von Mises Stress Within the Dies

In the present section, the stress distribution inside the CCDR dies is shown when the material is processed with the process conditions which are shown in Table 1. Figure 19 shows the nodes that have been analysed: node 1 corresponds with the inner radius, node 2 corresponds to the contact zone at the upper die before starting the angular channel and node 3 corresponds to the contact zone at the upper die after passing through the angular channel. It has been observed during the execution of the simulations that it is in these points where the sheet makes contact due to a lack of complete filling of the channel in the die.

As can be observed in Fig. 20, the point with the highest level of stress is that at the inner radius of the die, followed by the contact zone after passing through the intersection between both channels. The zone with the lowest value of stress is that at the upper part before the intersection zone between both channels since a big amount of the sheet surface rests over this.

In the image shown in Fig. 21, one can observe the von Mises stress inside the sheets when these are processed by CCDR. The obtained value is that from the material hardening law at the value of plastic deformation which it has accumulated at that moment.

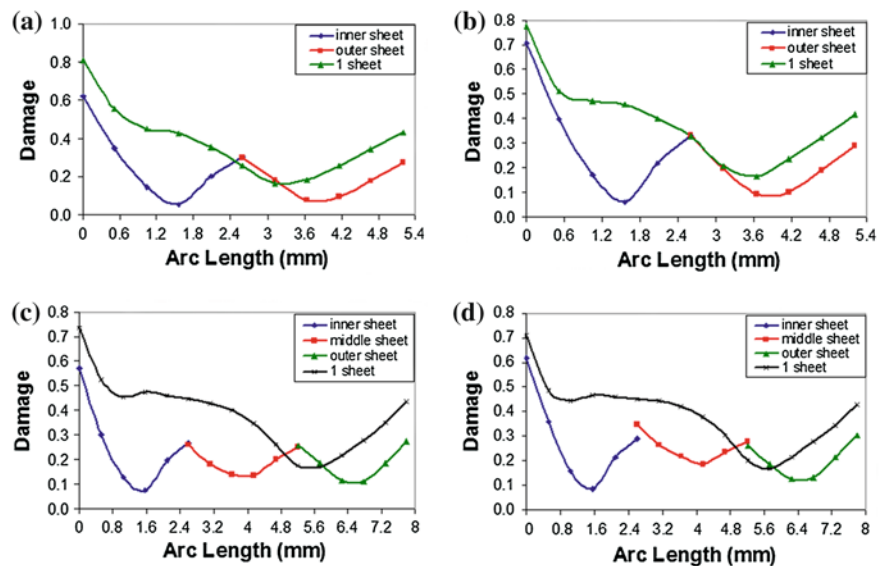


Fig. 17 Values of damage with Cockroft–Latham model in the sections of the sheets. **a** Damage pattern of one sheet of 4 mm thickness after being rolled versus two sheets processed simultaneously each one of 2 mm thickness with an inner radius of 2 mm. **b** Damage pattern of one sheet of 4 mm thickness after being rolled versus two sheets processed simultaneously each one of 2 mm thickness with an inner radius of 1.5 mm. **c** Damage pattern of one sheet of 6 mm thickness after being rolled versus three sheets processed simultaneously each one of 2 mm thickness with an inner radius of 2 mm. **d** Damage pattern of one sheet of 6 mm thickness after being rolled versus three sheets processed simultaneously each one of 2 mm thickness with an inner radius of 1.5 mm

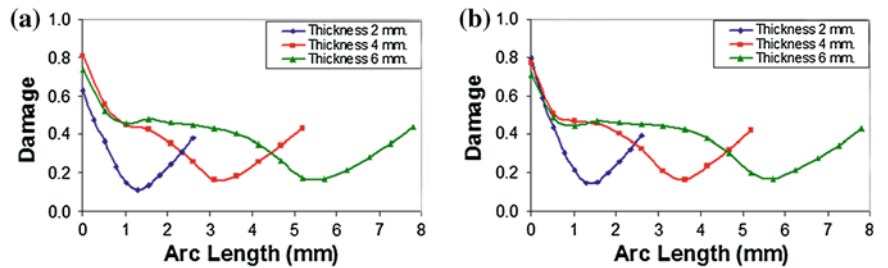


Fig. 18 Values of damage with Cockroft–Latham model in the sections of the sheets with different thickness. **a** Damage pattern for a single sheet with a thickness of 2 mm after being rolled **b** Damage pattern for a single sheet with a thickness of 4 mm after being rolled

Table 2 presents the results obtained from all the simulations which were carried out. It can be concluded that the most affected point when varying the inner radius is node 1, which, in general, presents the highest value of stress since it is at

Fig. 19 Nodes from which the information is taken during the CCDR process

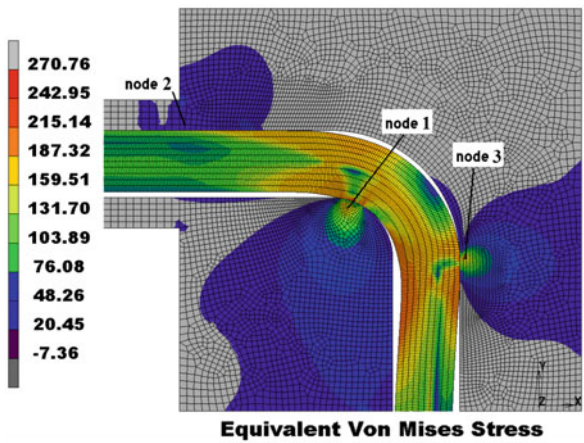
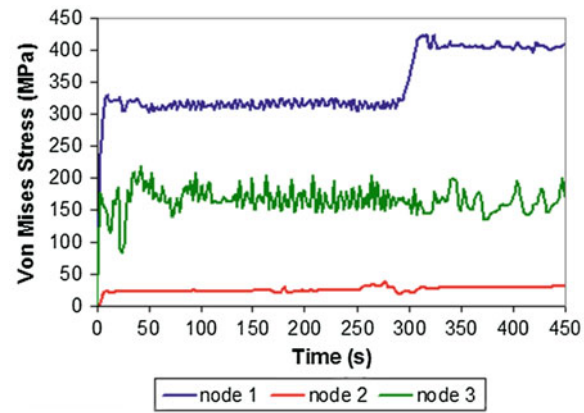


Fig. 20 Variation of von Mises stress during the CCDR process



this point that the sheet gets into contact in order to be deformed. When the inner radius decreases, the value of the von Mises stress is higher in the zone near the node 1, particularly for low values of the sheet thickness. For instance, for sheets with a thickness of 2.6 mm, changing a radius of 2 mm into a value of 1.5 mm means an increase in the stress of 10 %, in the case of a single sheet, and of 17.5 % in the case of two simultaneously processed sheets. Furthermore, when the sheet thickness is increased, the influence of the inner radius diminishes. Figure 22 shows a comparison between the values of stress that appear when a single sheet of 5.2 mm thickness is processed and those attained when two sheets with a thickness of 2.6 mm are processed.

As can be observed in Fig. 22, the stress variation inside the die at nodes 1 and 2 is negligible, whereas in the case of node 3, which corresponds with the outer part of the die, a considerable increase in the stress value is produced. The extreme case is given in the dies with an inner radius of 1.5 mm, where a stress peak

Fig. 21 Von Mises stress inside the sheets during the CCDR process

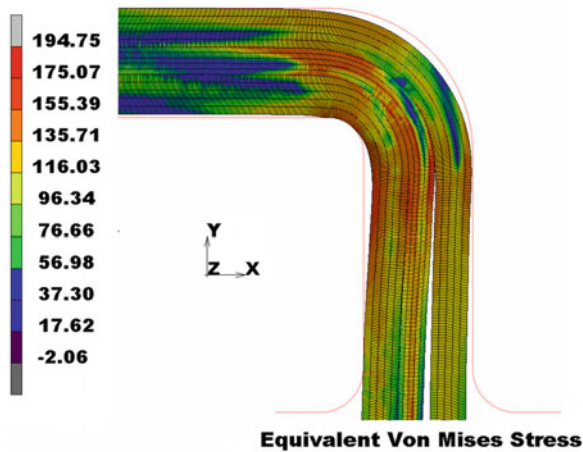


Table 2 Results of von Mises stress obtained from the different cases considered

Simulations	Node 1	Node 2	Node 3
1 sheet_2.6_2_2.2_90 %_rint2	297.1	30.5	279.4
1 sheet_2.6_2_2.2_90 %_rint1.5	337.8	39.4	254.7
1 sheet_5.2_4_4.2_90 %_rint2	423.1	38.6	216.7
1 sheet_5.2_4_4.2_90 %_rint1.5	427.1	77.0	172.4
1 sheet_7.8_6_6.2_90 %_rint2	410.0	52.2	112.3
1 sheet_7.8_6_6.2_90 %_rint1.5	426.8	56.1	107.3
2 sheets_5.2_4_4.2_90 %_rint2	404.2	24.3	234.5
2 sheets_5.2_4_4.2_90 %_rint1.5	470.1	23.0	392.3

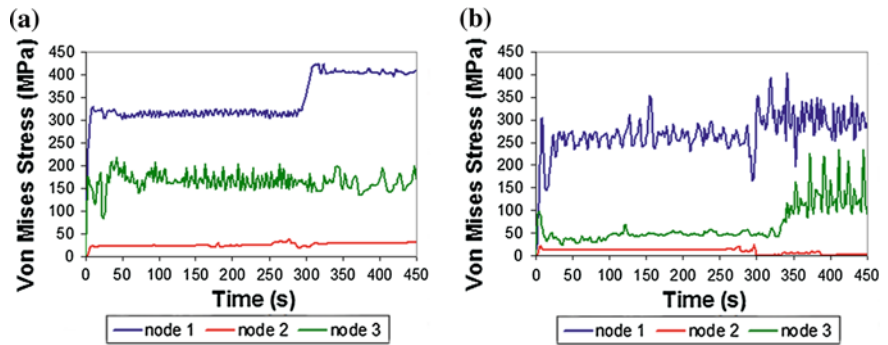


Fig. 22 Von Mises stress inside the sheets during the CCDR process. **a** Single sheet of 2 mm thickness after being rolled with a die of 2 mm inner radius. **b** Two sheets of 4 mm total thickness after being rolled with a die of 1.5 mm inner radius

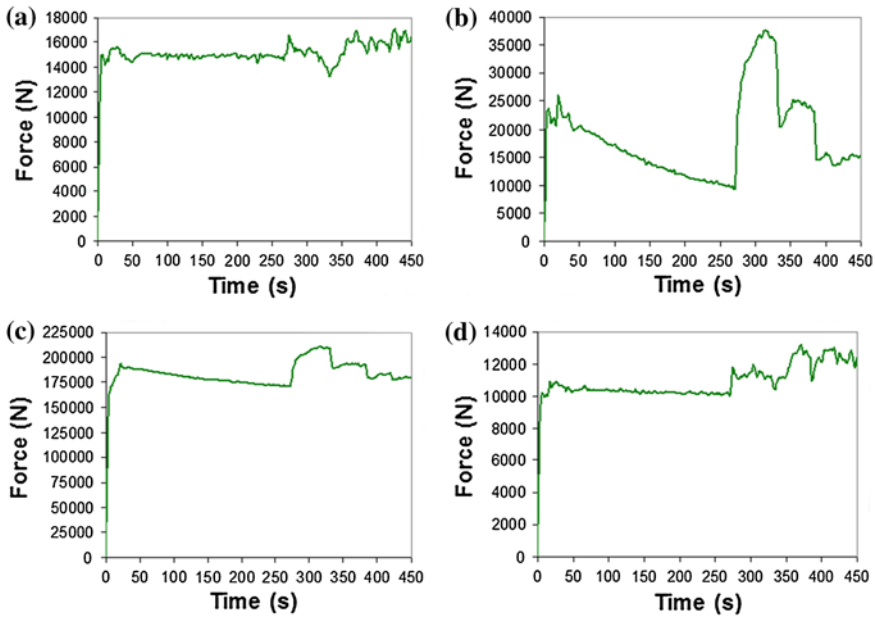


Fig. 23 Diverse forces involved in the CCDR process. **a** Force undergone by the lower die. **b** Force undergone by the upper die. **c** Pushing force carried out by a rolling mill. **d** Drawing force

appears doubling the value for the processing of a single sheet. This result may be due to the fact that with two sheets, a more efficient filling of the channel is produced.

4.4 Forces Required to Carry Out the CCDR Process

In the present section, the variation of the pushing force, the drawing force and those undergone by the CCDR dies is shown. In all cases, it is observed that when the rolled sheet starts to pass through the die (about 300 s), there are sudden changes in the forces and subsequently, there is an increase with respect to the non-rolled sheet part, which does not have accumulated plastic deformation. Figure 23 shows the graphs which correspond to a simulation with an initial sheet of 2.6 mm, rolling up to 2 mm, die channel of 2.2 mm and inner radius of 2 mm.

The force with the highest value involved in the CCDR process is the pushing force, which has to be multiplied by two since it represents the force of only one of the two rolls in the rolling mill.

The drawing force is the lowest of all and its value varies from 5 to 10 % of the pushing force. The values of the force undergone by the dies are counteracted with

Table 3 Forces required to carried out the CCDR process [N]

Simulations	Lower die	Upper die	Pushing force	Drawing force
1 sheet_2.6_2_2.2_90 %_rint2	17,057	37,553	210,285	13,182
1 sheet_2.6_2_2.2_90 %_rint1.5	21,959	41,388	215,981	14,712
1 sheet_5.2_4_4.2_90 %_rint2	51,889	53,141	256,096	31,191
1 sheet_5.2_4_4.2_90 %_rint1.5	50,805	52,668	260,135	31,177
1 sheet_7.8_6_6.2_90 %_rint2	77,131	59,680	292,586	56,998
1 sheet_7.8_6_6.2_90 %_rint1.5	76,402	59,349	293,456	58,112
2 sheets_5.2_4_4.2_90 %_rint2	25,388	17,118	222,796	19,640
2 sheets_5.2_4_4.2_90 %_rint1.5	30,503	22,840	229,451	21,261
3 sheets_7.8_6_6.2_90 %_rint2	43,459	26,788	237,727	37,530
3 sheets_7.8_6_6.2_90 %_rint1.5	43,542	27,250	239,217	39,281

the actual mechanical or hydraulic fasteners which allow us to compensate the force exerted by the material when this is deformed. The obtained results are presented in Table 3.

When the inner radius of the die is varied, no significant changes in the process forces are observed. For instance, when the value of the inner radius is reduced up to 1.5 mm, there is an increase of 15 % in the die forces, in the case of a single sheet with an initial thickness of 2.6 mm and in the case of two sheets with the previously mentioned value of thickness. The values of the force in the lower die decrease significantly when two sheets are processed in relation to those obtained when a single sheet with an equivalent thickness is processed, as is shown in Table 3. The same behaviour can be observed with the drawing force, although the decrease is lower. With respect to the pushing force, it is approximately the same.

From the results of the simulations, it can be stated that the values of the force when three sheets are processed by CCDR are the same as those obtained when a single sheet with a thickness equal to the three of them is processed. It is obvious that in order to reduce the values of the forces, it is better to process the three sheets at the same time. In this case, the clamping force of the dies is reduced by half, whereas the pushing force is reduced an average value of 15 % and the drawing force a 35 %.

The values of the drawing force and of the force undergone by the lower die are doubled when the values for the thickness of the processed sheet are doubled as well, that is to say, they follow approximately a linear law with the thickness. Nevertheless, the pushing force and the force undergone by the upper die increase approximately a 25 % when the sheet thickness is doubled.

5 Conclusions

In the present work, the results obtained from a study about a process denominated as Continuous Combined Drawing and Rolling (CCDR) have been shown. This study has been made by means of the finite element method and employing

different process conditions and different types of materials. This process is a new concept of severe plastic deformation processes (SPD), developed by researchers belonging to the Public University of Navarre and based on the patent (ES 2224787) [1]. With the results presented in this work, it is shown that this severe plastic deformation process is industrially viable and it is capable of operating in a continuous form, making it possible to manufacture highly deformed material.

Within the experimental section, it has been seen that the achievement of an optimum value of reduction in the rolling process is a determinant factor for the improvement in the mechanical properties. If the reduction is too high, the filling of the CCDD die is worse and the attained deformation is lower and less homogeneous, which limits the improvement in the mechanical properties of the material.

The decrease in the die inner radius, the processing of a single sheet and the increase in the thickness of the latter increase the deformation introduced in the material. As the improvement in the mechanical properties is linked to the plastic deformation introduced, the adequate selection of the angular channel die geometry will enable a greater improvement in the mechanical properties at each CCDD passage.

When the inner radius is decreased, the imparted damage is higher, especially for low values of sheet thickness. Another alternative in order to achieve a decrease in the level of damage is to process several sheets at the same time, since the mean value of damage in the section increases when the thickness of the processed sheet is increased.

The forces involved in the process increase their values when the inner radius is reduced and the sheet thickness is increased. Nevertheless, as it is the force carried out by the rolls of the rolling mill which is the highest from those involved in the CCDD process, it would be recommendable to increase the sheet thickness because this force increases in a much lower proportion than thickness.

Acknowledgments The authors acknowledge the support given by the Spanish Ministry of Science and Innovation Ministerio de Ciencia e Innovación Project No. MAT 2006-14341-C02-02.

References

1. Luis Pérez, C.J., González. P.A., Gil, J., Alkorta, J.: Procesado continuo de materiales metálicos mediante deformación plástica en canal poliangular. Pat. 2224787 (2002)
2. González, P.A., Luis Pérez, C.J., Garcés, Y., Gil Sevillano, J.: ECAE, una tecnología de procesado emergente para producir propiedades relevantes en materiales metálicos. *Rev. Metal.* **37**, 673–692 (2001)
3. Valiev, R.Z., Islamgaliev, R.K., Alexandrov, I.V.: Bulk nanostructured materials from severe plastic deformation. *Prog. Mater. Sci.* **45**, 103–189 (2000)
4. Yu, C.Y., Sun, P.L., Kao, P.W., Chang, C.P.: Mechanical properties of submicron-grained aluminum. *Scr. Mater.* **52**, 359–363 (2005)
5. Roven, H.J., Nesboe, H., Werenskiold, J.C., Seibert, T.: Mechanical properties of aluminium alloys processed by SPD: comparison of different alloy systems and possible product areas. *Mater. Sci. Eng. A* **410–411**, 426–429 (2005)

6. Xu, C., Furukawa, M., Horita, Z., Langdon, T.G.: Severe plastic deformation as a processing tool for developing superplastic metals. *J. Alloy. Compd.* **378**(1–2), 27–34 (2004)
7. Chen, H.H., Wang, J.Y., Lee, J., Lee, S.: Superplasticity of AA5083 alloy as processed by equal channel angular extrusión. *J. Alloy. Compd.* **460**, 305–308 (2008)
8. Segal, V.M.: Equal channel angular extrusion: from macromechanics to structure formation. *Mater. Sci. Eng. A* **271**, 322–333 (1999)
9. Luis Pérez, C.J.: On the correct selection of the channel die in ECAP processes. *Scr. Mater.* **50**, 387–393 (2004)
10. Luri, R., Luis, C.J.: Estudio por elementos finitos del proceso de extrusión en canal angular. 1er Congreso Internacional de la Sociedad de Ingeniería de Fabricación (CISIF 05), **1**, 1–8 (2005)
11. Luri, R., León, J., Luis, C.J., Puertas, I.: Mechanical behaviour of an Al–Mg alloy processed by ECAP. In: 21st International Manufacturing Conference (IMC 21), vol. 1, pp. 167–174 (2004)
12. Semiatin, S.L., Delo, D.P.: Equal channel angular extrusion of difficult-to work alloys. *Mater. Des.* **21**, 311–322 (2000)
13. Kim, H.S., Seo, M.H., Hong, S.I.: On the die corner gap formation in equal channel angular pressing. *Mater. Sci. Eng. A* **291**, 86–90 (2000)
14. Bowen, J.R., Gholinia, A., Roberts, S.M.: Analysis of the billet deformation behaviour in equal channel angular extrusión. *Mater. Sci. Eng. A* **287**, 87–99 (2000)
15. Tsai, T.L., Sun, P.L., Kao, P.W., Chang, C.P.: Microstructure and tensile properties of a commercial 5052 aluminum alloy processed by equal channel angular extrusión. *Mater. Sci. Eng. A* **342**, 144–151 (2003)
16. Sun, P.L., Cerreta, E.K., Gray, G.T., Rae, P.: The influence of boundary structure on the mechanical properties of ultrafine grained AA1050. *Mater. Sci. Eng. A* **410–411**, 265–268 (2005)
17. Wang, Z.C., Prangnell, P.B.: Microstructure refinement and mechanical properties of severely deformed Al–Mg–Li alloys. *Mater. Sci. Eng. A* **328**, 87–97 (2002)
18. Alkorta, J., Luis Pérez, C.J., Popova, E.N., Hafok, M., Pippan, R., Gil Sevillano, J.: Microstructure and indentation size-effect in pure niobium subjected to SPD via ECAP and HPT. *Mater. Sci. Forum.* **584–586**, 215–220 (2008)
19. Ferrasse, S., Segal, V.M., Alford, F., Kardokus, J., Strothers, S.: Scale up and Application of Equal Channel Angular Extrusion (ECAP) for the Electronics and Aerospace Industries. *Mater. Sci. Eng. A* **493**, 130–140 (2008)
20. Garcés, Y., Luis, C.J., Berlanga, C., González, P.: Equal channel angular extrusion in a commercial Al–Mn alloy. In: International Conference in Advances in Materials and Processing Technologies (AMPT'01), vol. 1, pp. 267–274 (2001)
21. González, P.A., Luis, C.J.: ECAP analysis of a 5083 Aluminium–Magnesium alloy. *Materials Congress* (2002)
22. Lugo, N., Cabrera, J.M., Llorca, N., Luis, C.J., Luri, R., León, J., Puertas, I.: Grain refinement of pure copper by ECAP. *Mater. Sci. Forum.* **584–586**, 393–398 (2008)
23. Kim, K.J., Yang, D.Y., Yoon, J.W.: Investigation of microstructure characteristics of commercially pure aluminum during equal channel angular extrusión. *Mater. Sci. Eng. A* doi:[10.1016/j.msea.2007.08.038](https://doi.org/10.1016/j.msea.2007.08.038) (2007)
24. Khan, Z.A., Chakkingal, U., Venugopal, P.: Analysis of forming loads, microstructure development and mechanical property evolution during equal channel angular extrusion of a commercial grade aluminum alloy. *J. Mater. Process. Technol.* **135**, 59–67 (2003)
25. Llorca Isern, N., Gonzalez, P.A., Luis, C.J., Laborde, I.: Severe plastic deformation of a commercial aluminium-lithium alloy (AA8090) by Equal Channel Angular Pressing. *Mater. Sci. Forum.* **503–504**, 871–876 (2006)
26. Segal, V.M.: Materials processing by simple shear. *Mater Sci Eng.* **197**, 157–164 (1995)
27. Lapovok, R., Loader, C., Dalla Torre, F.H., Semiatin, S.L.: Microstructure evolution and fatigue behavior of 2124 aluminum processed by ECAP with back pressure. *Mater. Sci. Eng. A* **425**, 36–46 (2006)

28. González PA., Luis CJ (2002) Severe Plastic Deformation by ECAP in an Al-Mg-Mn Commercial Alloy. 2nd Conference on SPD, NanoSPD2 1:251-256
29. Humphreys, F.J., Prangnell, P.B., Priestner, R.: Fine-grained alloys by thermomechanical processing. *Solid State Mater. Sci.* **5**, 15–21 (2001)
30. Huarte, B., Luis, C.J., Puertas, I., León, J., Luri, R.: Optical and mechanical properties of an Al–Mg alloy processed by ECAP. *J. Mater. Process. Technol.* **162–163**, 317–326 (2005)
31. Nakashima, K., Horita, Z., Nemoto, M., Langdon, T.G.: Development of multi-pass for equal-channel angular pressing to high total strains. *Mater. Sci. Eng. A* **281**, 82–87 (2000)
32. Neishi, K., Horita, Z., Langdon, T.G.: Grain refinement of pure nickel using equal-channel angular pressing. *Mater. Sci. Eng. A* **325**, 54–58 (2002)
33. Janecek, M., Popov, M., Krieger, M.G., Hellming, R.J., Estrin, Y.: Mechanical properties and microstructure of a Mg alloy AZ31 prepared by equal-channel angular pressing. *Mater. Sci. Eng. A* **462**, 116–120 (2007)
34. Shin, D.H., Seo, C.W., Kim, J., Park, K., Choo, W.Y.: Microstructures and mechanical properties of equal-channel angular pressed low carbon steel. *Scr. Mater.* **42**, 695–699 (2000)
35. Kaibyshev, R., Shipilova, K., Musin, F., Motohashi, Y.: Continuous dynamic recrystallization in an Al–Li–Mg–Sc alloy during equal-channel angular extrusion. *Mater. Sci. Eng. A* **396**, 341–351 (2005)
36. Nieh, T.G., Wadsworth, J., Sherby, O.D.: *Superplasticity in Metals and Ceramics*. Cambridge University Press, London (1997)
37. Li, C., Xia, Z., Sue, H.: Simple shear plastic deformation of polycarbonate plate II. Mechanical property characterization. *Polymer* **41**, 6285–6293 (2000)
38. Korbel, A., Richert, M.: Formation of shear bands during cyclic deformation of aluminium. *Acta Metall.* **33**, 1971–1978 (1985)
39. Richert, M., Stüwe, H.P., Zehetbauer, M.J., Richert, J., Pippan, R., Motz, Ch., Schafler, E.: Work hardening and microstructure of AlMg5 after severe plastic deformation by cyclic extrusion and compression. *Mater. Sci. Eng. A* **355**, 180–185 (2003)
40. Wang, Q.D., Chen, Y.J., Lin, J.B., Zhang, L.J., Zhai, C.Q.: Microstructure and properties of magnesium alloy processed by a new severe plastic deformation. *Mater. Lett.* **61**, 4599–4602 (2007)
41. Akbari Mousavi, S.A., Shahab, A.R., Mastoori, M.: Computational study of Ti-6Al-4 V flow behaviors during the twist extrusion process. *Mater. Des.* **29**, 1316–1329 (2008)
42. Vorhauer, A., Pippan, R.: On the homogeneity of deformation by high pressure torsion. *Scr. Mater.* **51**, 921–925 (2004)
43. Jiang, H., Zhu, Y.T., Butt, D.P., Alexandrov, I.V., Lowe, T.C.: Microstructural evolution, microhardness and thermal stability of HPT-processed Cu. *Mater. Sci. Eng. A* **290**, 128–138 (2000)
44. Sakai, G., Horita, Z., Langdon, T.G.: Grain refinement and superplasticity in an aluminum alloy processed by high-pressure torsion. *Mater. Sci. Eng.* **393**, 344–351 (2005)
45. Stolyarov, V.V., Zhu, Y.T., Lowe, T.C., Islamgaliev, R.K., Valiev, R.Z.: A two step SPD processing of ultrafine-grained titanium. *Nanostruct. Mater.* **11**, 947–954 (1999)
46. Sergueeva, A.V., Stolyarov, V.V., Valiev, R.Z., Mukherjee, A.K.: Advanced mechanical properties of pure titanium with ultrafine grained structure. *Scr. Mater.* **45**, 747–752 (2001)
47. Rajinikanth, V., Arora, G., Narasaiah, N., Venkateswarlu, K.: Effect of repetitive corrugation straightening on Al and Al-0.25 Sc alloy. *Mater. Lett.* **62**, 301–304 (2008)
48. Huang, J., Zhu, Y.T., Alexander, D.J., Liao, X., Lowe, T.C., Asaro, R.J.: Development of repetitive corrugation and straightening. *Mater. Sci. Eng. A* **371**, 35–39 (2004)
49. Ghosh, A.K., Huang, W.: Severe deformation based process for grain subdivision and resulting microstructures. *Invest. appl. Severe Plast. Deformation* **1**, 29–36 (2000)
50. Valiev, R.Z., Langdon, T.G.: Principles of equal-channel angular pressing as a processing tool for grain refinement. *Prog. Mater. Sci.* **51**, 881–981 (2006)
51. Zhu, Y.T., Lowe, T.C., Langdon, T.G.: Performance and applications of nanostructured materials produced by severe plastic deformation. *Scr. Mater.* **51**, 825–830 (2004)

52. Latysh, V., Krallics, G.Y., Alexandrov, I., Fodor, A.: Application of bulk nanostructured materials in medicine. *Curr. Appl. Phys.* **6**, 262–266 (2006)
53. Tanaka, T., Makii, K., Ueda, H., Kushibe, A., Kohzu, M., Higashi, K.: Study on practical application of a new seismic damper using a Zn–Al alloy with a nanocrystalline microstructure. *Int. J. Mech. Sci.* **45**, 1599–1612 (2003)
54. Luis Pérez, C.J., León Iriarte, J.: Fem simulation of the continuous combined drawing and rolling pressing in equal channel angular (CCDR-ECAP). *UFG3* **1**, 205–210 (2004)
55. Luis Pérez, C.J., León Iriarte, J., Díaz de Rada, C.: A method for continuous processing of materials by equal channel angular extrusion processes. In: *International Conference on Advanced Materials and Processing Technologies, AMPT'03*, vol. 1, pp. 1162–1165 (2003)
56. Cockroft, M.G., Latham, D.J.: Ductility and the workability of metals. *Inst. Met.* **96**, 33–39 (1968)
57. Marc.: R1, Theory and User information A (2008)
58. Lemaitre, J.: *A Course on Damage Mechanics*. Springer, New York (1996)
59. Bonora, N., Ruggiero, A., et al.: Practical applicability and limitations of the elastic modulus degradation technique for damage measurements in ductile metals. *Strain* (2010). doi:10.1111/j.1475-1305.2009.00678.x
60. Gurson, A.L.: Continuum theory of ductile rupture by void nucleation and growth: part I—Yield criteria and flow rules for porous ductile media. *J. Eng. Mat. Tech.* **99**, 2–15 (1977)
61. Kachanov, L.M.: On creep rupture time. *Izv. Acad. Nauk SSSR, Otd. Techn. Nauk* **88**, 26–31 (1958)
62. Lemaitre, J.: A continuous damage mechanics model for ductile fracture. *J. Eng. Mat. Tech.* **107**, 83–89 (1985)
63. Murakami, S.: Damage mechanics approach to damage and fracture of materials. *Rairo* **3**, 1–13 (1982)
64. Krajcinovic, D.: Damage mechanics. *Mech. Mat.* **8**, 117–197 (1989)
65. Bonora, N., Gentile, D., et al.: Ductile damage evolution under triaxial state of stress: theory and experiments. *Int. J. Plast.* **21**, 981–1007 (2005)
66. Needleman, A., Tvergaard, V.: An analysis of ductile rupture in biaxially stretched sheets. *J. Eng. Mat. Tech.* **102**, 249–256 (1984)
67. Gao, X., Faleskog, J., Shih, C.F., Dodds, R.H.J.: Ductile tearing in part-through cracks: experiments and cell-model predictions. *Eng. Fract. Mech.* **59**, 761–777 (1998)
68. Chaboche, J.L.: Anisotropic creep damage in the framework of the continuum damage mechanics. *Nucl. Eng. Des.* **79**, 309–319 (1984)
69. Bonora, N.: A non-linear CMD damage model for ductile failure. *Eng. Fract. Mech.* **58**, 11–28 (1997)
70. Luri, R., Luis Pérez, C.J., et al.: Evolution of damage in AA-5083 processed by equal channel angular extrusion using different die geometries. *J. Mater. Process. Technol.* **211**, 48–56 (2011)

Numerical Modeling of Materials Under Extreme
Conditions

Bonora, N.; Brown, E.N. (Eds.)

2014, VI, 230 p. 147 illus., 123 illus. in color., Hardcover

ISBN: 978-3-642-54257-2